



HAL
open science

Interferometric observations of the supergiant stars alpha Orionis and alpha Herculis with FLUOR at IOTA

Guy Perrin, Stephen Ridgway, Vincent Coudé Du Foresto, Bertrand
Mennesson, Wesley A. Traub, M. G. Lacasse

► **To cite this version:**

Guy Perrin, Stephen Ridgway, Vincent Coudé Du Foresto, Bertrand Mennesson, Wesley A. Traub, et al.. Interferometric observations of the supergiant stars alpha Orionis and alpha Herculis with FLUOR at IOTA. *Astronomy and Astrophysics - A&A*, 2004, 418, pp.675-685. 10.1051/0004-6361:20040052 . hal-03742374

HAL Id: hal-03742374

<https://hal.science/hal-03742374>

Submitted on 9 Sep 2022

HAL is a multi-disciplinary open access archive for the deposit and dissemination of scientific research documents, whether they are published or not. The documents may come from teaching and research institutions in France or abroad, or from public or private research centers.

L'archive ouverte pluridisciplinaire **HAL**, est destinée au dépôt et à la diffusion de documents scientifiques de niveau recherche, publiés ou non, émanant des établissements d'enseignement et de recherche français ou étrangers, des laboratoires publics ou privés.

Interferometric observations of the supergiant stars α Orionis and α Herculis with FLUOR at IOTA[★]

G. Perrin¹, S. T. Ridgway², V. Coudé du Foresto¹, B. Mennesson³, W. A. Traub⁴, and M. G. Lacasse⁴

¹ Observatoire de Paris, LESIA, UMR 8109, 92190 Meudon, France

² National Optical Astronomy Observatories, Tucson, AZ 85726-6732, USA

³ Jet Propulsion Laboratory, California Institute of Technology, MS 306-388, 4800 Oak Grove Drive, Pasadena, CA 91109, USA

⁴ Harvard-Smithsonian Center for Astrophysics, Cambridge, MA 02138, USA

Received 3 February 2003 / Accepted 30 January 2004

Abstract. We report the observations in the K band of the red supergiant star α Orionis and of the bright giant star α Herculis with the FLUOR beamcombiner at the IOTA interferometer. The high quality of the data allows us to estimate limb-darkening and derive precise diameters in the K band which combined with bolometric fluxes yield effective temperatures. In the case of Betelgeuse, data collected at high spatial frequency although sparse are compatible with circular symmetry and there is no clear evidence for departure from circular symmetry. We have combined the K band data with interferometric measurements in the L band and at $11.15 \mu\text{m}$. The full set of data can be explained if a 2055 K layer with optical depths $\tau_K = 0.060 \pm 0.003$, $\tau_L = 0.026 \pm 0.002$ and $\tau_{11.15 \mu\text{m}} = 2.33 \pm 0.23$ is added $0.33 R_\star$ above the photosphere providing a first consistent view of the star in this range of wavelengths. This layer provides a consistent explanation for at least three otherwise puzzling observations: the wavelength variation of apparent diameter, the dramatic difference in limb darkening between the two supergiant stars, and the previously noted reduced effective temperature of supergiants with respect to giants of the same spectral type. Each of these may be simply understood as an artifact due to not accounting for the presence of the upper layer in the data analysis. This consistent picture can be considered strong support for the presence of a sphere of warm water vapor, proposed by Tsuji (2000) when interpreting the spectra of strong molecular lines.

Key words. stars: supergiants – infrared: stars – techniques: interferometric

1. Introduction

Because of their large luminosity supergiant stars have extended atmospheres, with resultant low surface gravity and large pressure scale height. The cool supergiants are usually slightly variable in brightness, color, polarization, and radial velocity, suggestive of significant dynamic and radiative activity and inhomogeneities. However, the variability is small enough that static model atmospheres are normally considered adequate for abundance studies. Owing to the very extended atmospheres, and in some cases circumstellar shells, it is difficult to determine even some very basic parameters for these stars. Here, we address the question of the effective temperatures. The near infrared wavelength regime offers several advantages for the study of cool supergiants – it is less obscured by scattering and line blanketing (problems in the visible) and by dust (detected in the mid-infrared).

α Orionis is a bright, prototypical example of the cool supergiant class. It is classified M1-2Ia-Iab, which places it firmly in the supergiant category. An infrared excess and extended dust shell confirm substantial mass loss. α Orionis has been observed several times with high angular resolution techniques and in several optical bandpasses. The derived angular diameters are plotted against wavelength in Fig. 1. The observed angular diameters are significantly larger in the visible, decrease to a minimum in the near-infrared, and then increase again in the mid-infrared. Some surface structure, similar to large spots, has been seen at several wavelengths in the red (Tuthill et al. 1997; Young et al. 2000). These spots have not been seen at other nearby wavelengths.

We have observed α Orionis in the K band with FLUOR at IOTA in 1996 and 1997. We will present these observations in the next section and explain the data reduction procedure. In the following sections we will derive uniform disk, limb darkened and linear diameters. We will compare our results to the previous observations and derive a simple model for the wavelength dependence of diameters in Sect. 6. We also present similar observations of α Herculis. α Herculis has been classified

Send offprint requests to: G. Perrin,

e-mail: guy.perrin@obspm.fr

[★] Based on observations collected at the IOTA interferometer, Whipple Observatory, Mount Hopkins, Arizona.

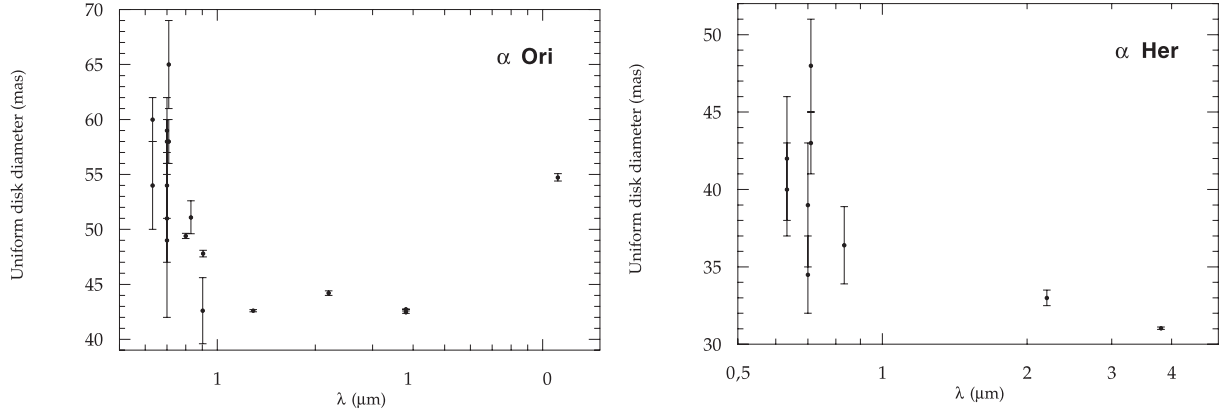


Fig. 1. Uniform disk diameters measured for α Orionis and α Herculis. Values are reported in Benson et al. (1991), Mozurkewich et al. (1991), Dyck et al. (1992), Tuthill et al. (1997), Burns et al. (1997), Mennesson et al. (1999), Young et al. (2000), Weiner et al. (2000), Chagnon et al. (2002).

Table 1. Log of observations.

Source	Date	Band	Spatial frequency (cycles/arcsec)	Position angle ($^{\circ}$)	Visibility	Reference 1	Reference 2
α Orionis	18/02/1996	<i>K</i>	44.08	–	0.0843 ± 0.0024	HD 18884	HD 94705
	9/11/1996	<i>K</i>	24.43	63.01	0.1253 ± 0.0016	HD 18884	HD 42995
	9/11/1996	<i>K</i>	23.34	71.96	0.1847 ± 0.0024	HD 18884	HD 42995
	9/11/1996	<i>K</i>	22.70	80.47	0.2045 ± 0.0020	HD 44478	HD 44478
	9/11/1996	<i>K</i>	22.50	85.91	0.2232 ± 0.0018	HD 44478	HD 44478
	22/02/1997	<i>K</i>	64.96	79.06	0.0510 ± 0.0010	HD 61421	HD 61421
	9/03/1997	<i>K</i>	42.81	69.89	0.0949 ± 0.0047	–	HD 61421
α Herculis	17/04/1996	<i>K</i>	35.67	53.97	0.0800 ± 0.0038	HD 89758	HD 186791
	17/04/1996	<i>K</i>	35.26	59.28	0.0894 ± 0.0022	HD 89758	HD 186791
	21/04/1996	<i>K</i>	46.57	106.31	0.0954 ± 0.0068	HD 130144	–
	6/03/1997	<i>K</i>	35.05	60.90	0.1072 ± 0.0028	HD 130144	–
	6/03/1997	<i>K</i>	35.51	57.07	0.0927 ± 0.0027	HD 130144	–

M51b-II, indicative of a somewhat lower luminosity. It does not have an infrared excess. Previously determined diameters are also plotted in Fig. 1.

2. Observations and data reduction

The stars have been observed in 1996 and 1997 with the IOTA (Infrared-Optical Telescope Array) interferometer located at the Smithsonian Institution's Whipple Observatory on Mount Hopkins, Arizona (Traub et al. 1998). Several baselines of IOTA have been used to sample visibilities at different spatial frequencies. The data have been acquired with FLUOR (Fiber Linked Unit for Optical Recombination) in the *K* band. Beam combination with FLUOR is achieved by a single-mode fluoride glass triple coupler in the *K* band. The fibers spatially filter the wavefronts corrugated by the atmospheric turbulence. The phase fluctuations are traded against photometric fluctuations which are monitored for each beam to correct for them a posteriori. At the time of the reported observations the modulation of the optical path difference was produced by scanning through the fringe packet with the IOTA short delay line and the four signals were detected with InSb single-pixel detectors (Perrin 1996). The limiting magnitude was then $K = 0$. The accuracy

on visibility estimates measured by FLUOR is usually better than 1% for most sources (Perrin et al. 1998).

The log of the observations is given in Table 1. The second column is the UT date of the observations. The next two columns are the spatial frequency and the position angle of the spatial frequency vector. The next column is the visibility and the 1σ error. The last two columns are the HD numbers of the reference sources observed just before and just after the science target to estimate the instrumental visibility. The characteristics of the reference sources (spectral type and uniform disk diameter) are listed in Table 2. Diameters have either been measured or derived from photometric and spectroscopic scales (Cohen et al. 1996; Perrin et al. 1998). Each line in Table 1 corresponds to two batches of data: the signals acquired on-source (the fringes) representing a collection of at least 100 scans; the signals acquired off-source to estimate the contribution of the detector to the noise (same number of scans) in the *K* band. These two batches are called an observation block. The same sequences are repeated for the reference stars.

The procedure explained in Coudé du Foresto et al. (1997) has been applied to all sources independently to estimate the average contrast of the fringe packet for each observation block. The expected visibility of the calibrators is then

Table 2. Reference sources.

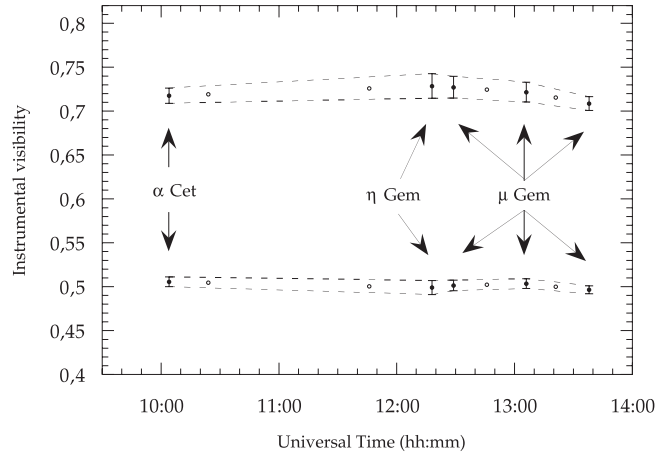
HD number	Source name	Spectral type	Uniform disk diameter (mas)
HD 18884	α Cet	M 1.5 III	12.66 ± 0.36^a
HD 94705	56 Leo	M 5.5 III	8.66 ± 0.43^b
HD 42995	η Gem	M 3 III	10.64 ± 0.53^b
HD 44478	μ Gem	M 3 III	13.50 ± 0.15^c
HD 61421	α CMi	F 5 IV	5.25 ± 0.26^b
HD 89758	μ UMa	M 0 III	8.28 ± 0.41^b
HD 186791	γ Aql	K 3 II	6.99 ± 0.35^b
HD 130144	HR 5512	M 5 III	8.28 ± 0.41^b

^a Cohen et al. (1996).^b Photometric estimate.^c Di Benedetto & Rabbia (1987).

computed at the time they were observed. The instrumental visibility is then interpolated at the time when the science targets have been observed. Division of the fringe contrast of the science targets by the interpolated instrumental visibility provides the final visibility estimate. This procedure has been explained in Perrin et al. (1998). It has been recently refined (Perrin 2003a) to take into account correlations in fringe contrast estimates and transfer function estimates in the computation of error bars. In the special case of the February 18th, 1996 K band observation, the triple coupler was not available and we had to use a single coupler instead. The only difference is that no photometric signals are available. Instead, the low frequency part of the interferograms is used to estimate the photometric fluctuations. The calibration is therefore less accurate than with the triple coupler and the possibility of bias in the final visibility estimate must be considered. However, the bias being proportional to the visibility is more important when the average intensities in the two interferometric arms are not well balanced. In the case of this particular observation, the visibility is low and the two arms were well balanced. For these reasons the bias is negligible and the data are retained.

A manual correction of the bias of the squared fringe contrast by the source photon noise has been added to the regular procedure of data reduction for the K band data. At the time when InSb detectors were used, the sensitivity of FLUOR was so low ($K = 0$) that the bias due to photon noise could usually be neglected. Yet, on very bright sources like α Orionis and α Herculis, the bias is larger than the tiny error bars achieved and its correction is mandatory for best results. The general expression of the photon noise bias is well described in Goodman (1985). This expression can be adapted in the case of FLUOR giving the theoretical value of the bias that has to be removed from the data (Perrin 2003b). When the conversion factor between ADUs (or detector output voltage) and photons is well known, the removal of the bias is easy and can be automated. This is not unfortunately the case for the data presented in this paper and this is why the procedure had to be manual.

To illustrate the great stability of the FLUOR measurements in the K band, the instrumental visibility for November 9, 1996 has been plotted in Fig. 2 for the two

**Fig. 2.** Instrumental visibility on November 9, 1996 for the two interferometric channels (full circles). Open circles are the interpolated instrumental visibilities at the time Betelgeuse was observed.

interferometric channels. The dashed lines represent the 1σ lower and upper limits. Three different calibrators have been used and the transfer function is stable to better than 1σ on a time scale of 2 h. The interpolation of the transfer function to the time of the observation of the science target (open circles) therefore yields a very accurate estimate of the visibility transfer function.

3. Uniform disk diameters

3.1. Wide band V^2 visibility models

The bandwidth of the K band is about 400 nm inducing a spread of spatial frequencies for each individual measurement. This spread is nearly negligible when the average spatial frequency is small, as is the case for spatial frequencies in the first lobe of the visibility function. At higher spatial frequencies the spread increases and its influence keeps increasing as the visibility model is no longer monotonic. The averaging of visibilities across the bandpass cannot be neglected. Under conditions of turbulence and without a fringe tracking system to stabilize differential piston between the two pupils, interferograms are distorted and the fringe peak is spread leading to a mixing of frequencies. This raises the issue of whether one should average complex visibilities and square the result or directly average squared visibilities to compute the wide band visibility model. It is not the purpose of this paper to discuss this and this point will be tackled in a forthcoming paper. It can be shown that for the data discussed here it is legitimate to average the squared monochromatic visibilities.

Models for which the squared visibility is averaged over the K band have been computed. The monochromatic components are weighted by the K band filter transmission and by the spectrum of the source which has been modeled by a 3500 K black-body Planck function. The chromatic splitting ratios of the recombining coupler have also been taken into account as wavelengths for which the coupler is 50/50 contribute more to the average visibility than those for which the coupler is unbalanced. Splitting ratios have been estimated from narrow band

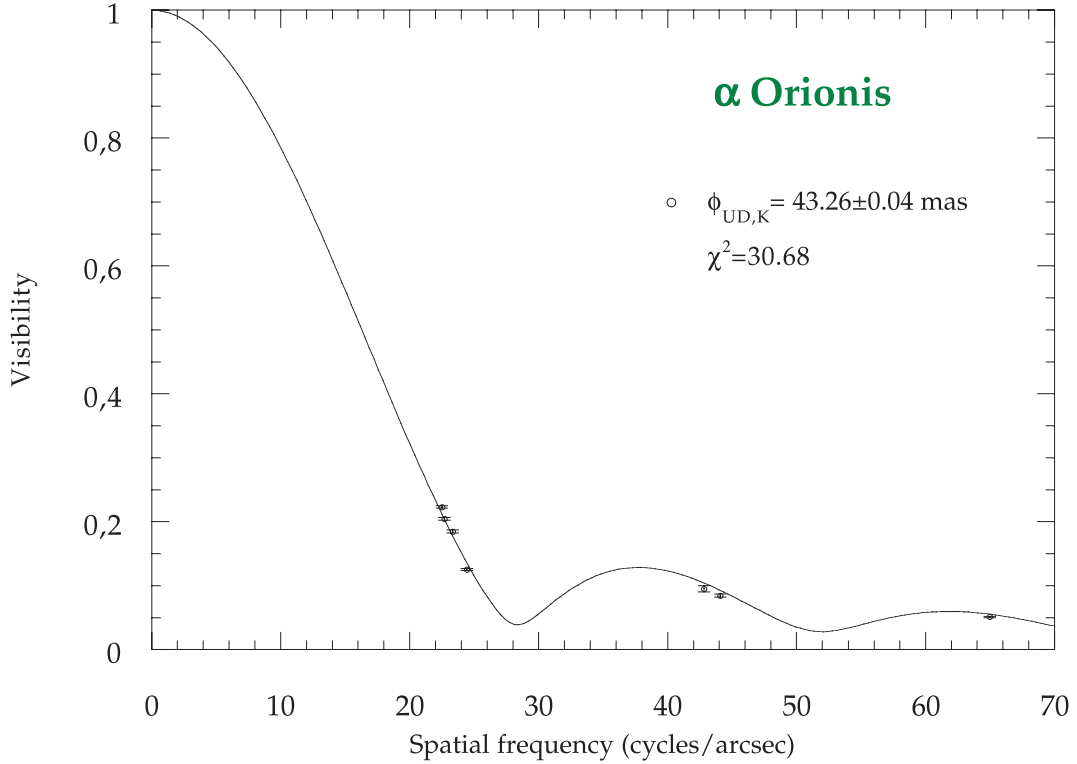


Fig. 3. K band visibilities for α Orionis. The χ^2 is computed with first lobe visibilities only.

measurements. The maxima of the averaged visibility function are smaller than the maxima of a monochromatic visibility model thus mimicking a limb darkening effect. Besides the zeroes of the monochromatic visibility function are replaced by minima of a few percent. It is therefore important to take averaging into account.

3.2. Model fitting

The visibility data have been fitted by a wide band uniform disk diameter visibility curve by minimizing the function:

$$\chi^2 = \frac{1}{N-1} \sum_{i=1}^N \left(\frac{V_i^2 - M(\varnothing_{UD}; S_i)}{\sigma_i} \right)^2 \quad (1)$$

where σ_i is the estimated error on V_i^2 and:

$$M(\varnothing_{UD}; S_i) = \int_{\text{band}} \left| \frac{2J_1(\pi\varnothing_{UD}B_ik)}{\pi\varnothing_{UD}B_ik} \right|^2 w(k) dk \quad (2)$$

is the wide band uniform disk model with k the wavenumber, $S_i = B_ik_{\text{eff}}$ the effective spatial frequency, B_i the projected baseline and \varnothing_{UD} the uniform disk diameter, $w(k)$ being a weighting function.

If the model is a perfect representation of the source and if the error bars are well estimated then the mean of χ^2 is equal to 1. The value of the χ^2 can therefore be used as a criterion to assess the validity of the error bar estimates.

The K band visibility data of α Orionis have been gathered and fitted by a single visibility function. The 1996 and 1997 K band data for α Herculis are fitted separately. We present the results of the fits for the first lobe data only (spatial

frequency ≤ 30 and 40 cycles/arcsec for α Orionis and α Herculis respectively) and for all data points. The results are the following for all epochs:

α Orionis

$$\varnothing_{UD, 1st} = 43.26 \pm 0.04 \text{ mas} \quad \chi^2 = 30.68$$

$$\varnothing_{UD, all} = 43.33 \pm 0.04 \text{ mas} \quad \chi^2 = 21.45$$

α Herculis

$$\varnothing_{UD, 1996, 1st} = 31.66 \pm 0.08 \text{ mas} \quad \chi^2 = 0.004$$

$$\varnothing_{UD, 1996, all} = 31.64 \pm 0.08 \text{ mas} \quad \chi^2 = 3.37$$

$$\varnothing_{UD, 1997} = 31.24 \pm 0.07 \text{ mas} \quad \chi^2 = 0.85.$$

The data are presented in Figs. 3 and 4, with the uniform disk model fits. The agreement of the first lobe data of α Herculis to the model is virtually “perfect”, setting the upper level of accuracy of the FLUOR data to 0.2%, and confirming that the measurement error bars are reasonable. This conclusion has also been verified on other bright stars. Despite the correctness of the error bar estimates, the accuracy of the diameter measurements may be questionable. As a matter of fact the diameter estimates depend on the estimated effective wavelength of the instrument and are directly proportional to it. The direct measurement of the effective wavelength is quite difficult and depends on a large number of parameters. We have assessed the quality of our diameter estimates by comparing them to some independent measurements in the paragraph 4.5.3 of Perrin et al. (1998). The diameters of α Boo and α Tau measured with an accuracy of 1 part in 200 with FLUOR were statistically compatible with measurements obtained at the same or different wavelengths with other interferometers or by the lunar occultation technique. In the case of α Orionis and

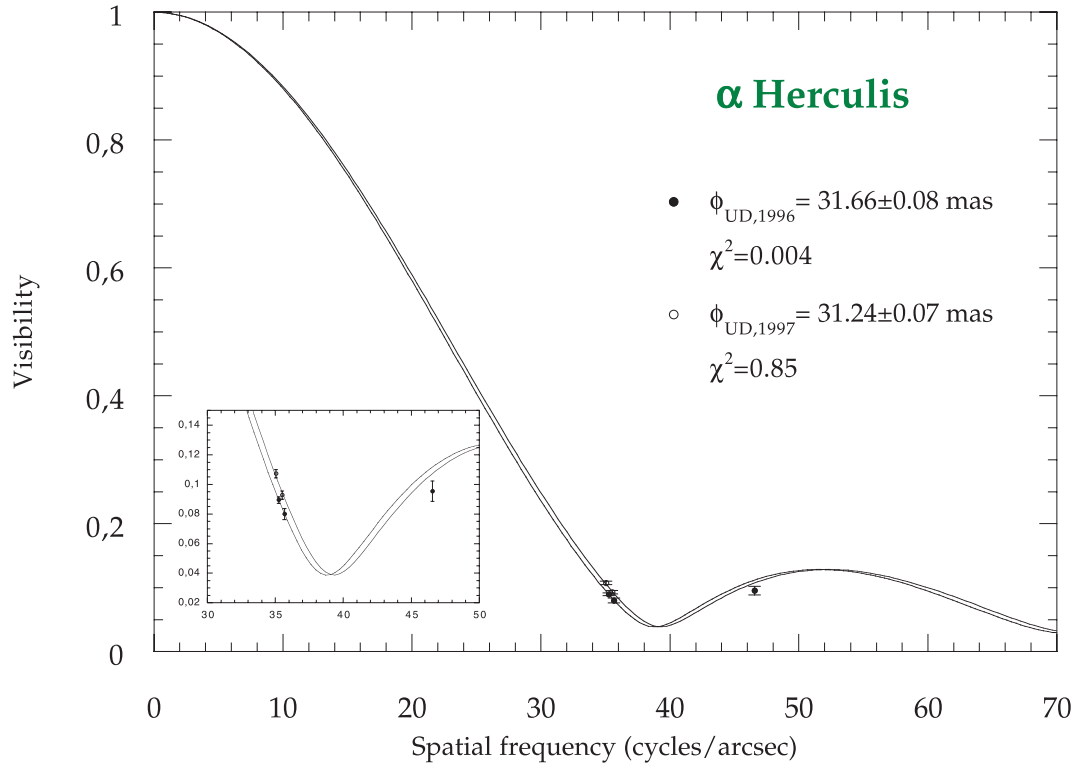


Fig. 4. K band visibilities for α Herculis. The χ^2 is computed with first lobe visibilities only.

α Herculis we are therefore confident in our diameter estimates at least at the level of 1 part in 200. With this understanding, the data in Figs. 3 and 4 suggest or confirm several conclusions.

First, the consistency of the observations and the small error bars with the simple model suggests that the surface of α Herculis is well behaved, in some sense – there is no evidence here for a substantial surprise.

Second, there has probably been a slight change of apparent diameter of 0.4 milli-arcsec between April 1996 and March 1997 as Fig. 4 shows. This is evidently a small effect, but is clearly indicated by the data at the level of precision which is believed to apply. For such a small effect however, it is not clear if the photospheric radius has actually changed, or if an opacity or temperature variation has changed the brightness profile slightly.

Third, in the case of Betelgeuse, we immediately see that the data do not fit the simple model as well. There may be a calibration problem. Yet, we wish to suggest a possible alternative explanation to this issue. It appears that the surface of the star cannot be considered smooth and the brightness distribution must have some roughness. In fact such an effect has been predicted to be in the range of 0.1 to 1% (Von der Luhe 1997) depending on the spectral type of the star. This roughness of the visibilities may thus induce large values of χ^2 , and the fit may be very sensitive to which visibility values are included. To illustrate this, the point with $S = 24.43$ cycles/arcsec seems slightly inconsistent with the three other first lobe data points. Without this visibility point, the χ^2 of the fit with the first lobe points is 7.70 and becomes 15.00 if second and third lobe data

points are added. The statistics are thus significantly changed and are therefore fragile.

The fourth conclusion to be drawn is that the full range of visibility data for each star is in neither case consistent with a uniform disk model. This means that limb darkening has to be taken into account, as discussed in the next section.

4. Physical diameters

Discrepancies between the uniform disk and limb darkened disk models mostly occur after the first zero of the visibility function. Data in the K band have been obtained in this range of spatial frequencies and must take limb darkening effects into account. Wide band chromatic effects need also to be taken into account to properly estimate the limb darkening parameters.

4.1. Limb darkening measurements on α Orionis and α Herculis

Several limb darkening models have been published. With a limited number of data points available for the two stars, only single parameter models are used. We have adopted the classical linear limb darkening model and the power law model as proposed by Hestroffer (1997). These can be expressed as:

$$I(\mu) = 1 - A(1 - \mu) \quad (3)$$

$$I(\mu) = \mu^\alpha \quad (4)$$

where μ is the cosine of the angle between the line of sight and the vector joining the current point to the center of the star. The intensity is normalized with respect to the center of the stellar surface.

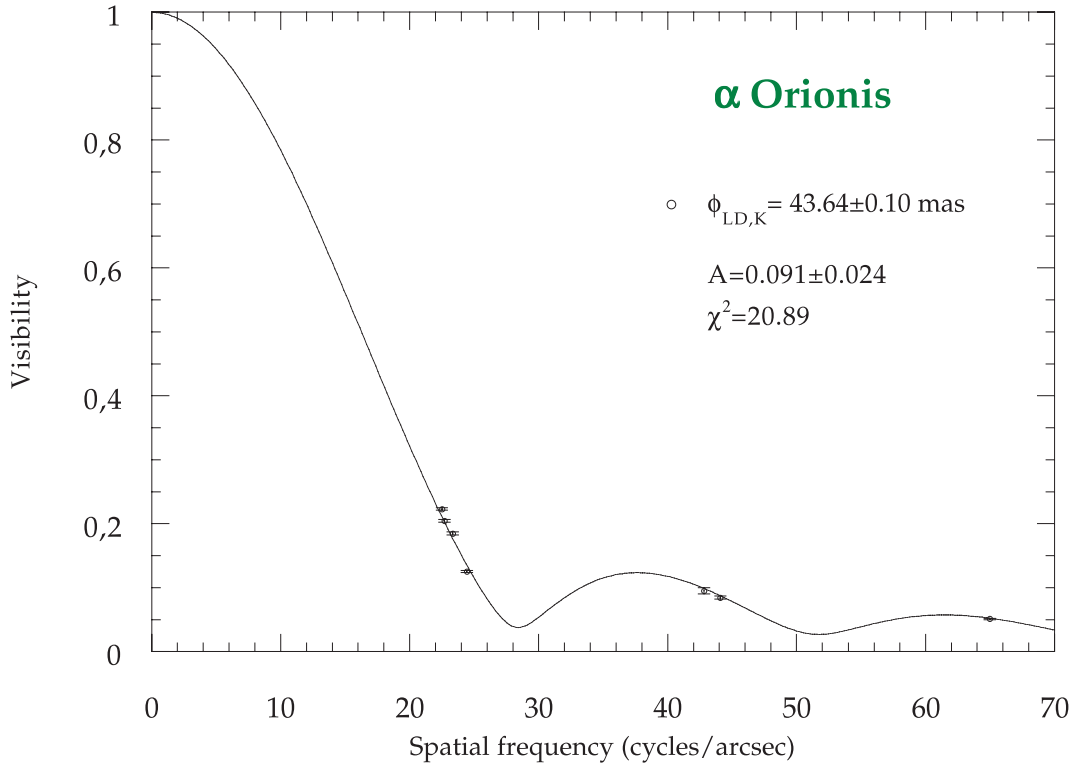


Fig. 5. Fit of α Orionis data by a limb darkened disk model.

4.1.1. α Herculis

Only the 1996 data are used since no data were taken in the second lobe in 1997. The results of the fit are listed in the table below:

Model	Diameter (mas)	Parameter	Reduced χ^2
Power	33.59 ± 0.89	0.394 ± 0.180	0.016
Linear	33.14 ± 0.76	0.429 ± 0.176	0.016

The fitting residuals are smaller than with a uniform disk model and both limb darkening models yield the same diameter. The limb darkening parameter is clearly determined in both cases. There is a 6% increase between the uniform disk model and the limb darkened disk model.

Unfortunately no physical value for the α parameter of the power law has been predicted. For the linear law, Van Hamme (1993) has predicted a coefficient of 0.321 for a star with an effective temperature of 3500 K and a surface gravity of $\log g = 0.5$. For the same set of physical parameters, Claret (2000) predicts a coefficient of 0.436. Our measurement is therefore in excellent agreement with both predictions, but cannot distinguish between them.

4.1.2. α Orionis

The same two models were applied to the α Orionis data. The results are reported below:

Model	Diameter (mas)	Parameter	Reduced χ^2
Power	43.76 ± 0.12	0.071 ± 0.018	20.7
Linear	43.65 ± 0.10	0.090 ± 0.025	20.9

The results of the fits are displayed in Figs. 5 and 6. The reduced χ^2 are lower than the one obtained with a uniform disk model showing that taking into account a limb darkening effect improves the fitting of the data. Both parameters are well constrained by the data. Yet, the coefficient of the linear model is much smaller than the ones predicted by the above cited authors as opposed to what has been found for α Herculis. The surface of Betelgeuse would therefore be far less limb darkened than that of α Herculis, which may be surprising for stars with similar spectral types. The increase in physical diameter due to the limb darkening effect is only of 1%. Errors on the physical parameters of Betelgeuse can hardly be invoked as the linear law coefficient computed from models does not seem to vary much in a wide range of surface gravity and temperature values. A calibration error in the data is not a plausible explanation. The highest frequency point in the first lobe is obviously introducing the largest error in the fit and is very constraining as it is located closer to the null. Removing this point doubles the linear coefficient and does not change the diameter. In any case this is not sufficient to change the conclusion. Assuming that the number of points is sufficient to constrain well the single parameter limb darkening profile of Betelgeuse, we report that the effect is much smaller in the K band than predicted.

4.2. Linear radii

Using the HIPPARCOS parallaxes published by Perryman et al. (1997) linear radii can be derived for both stars (we have used the formulas by Browne (2002) to compute the error for

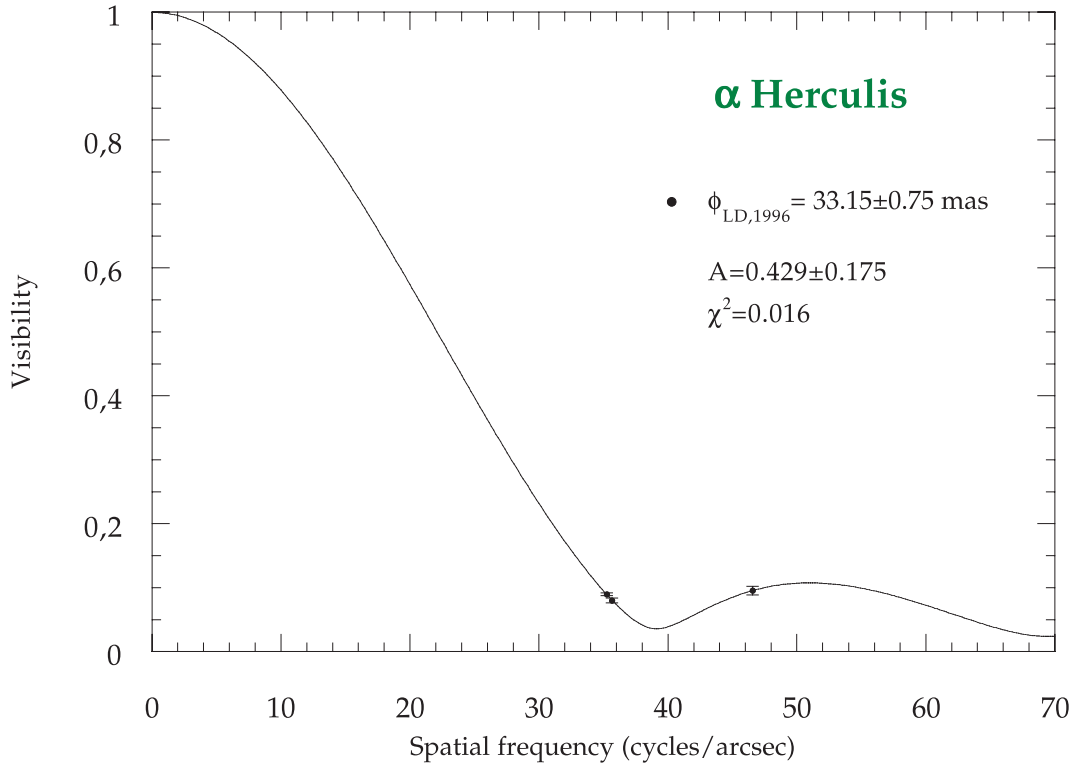


Fig. 6. Fit of 1997 α Herculis data by a limb darkened disk model.

the ratio of Gaussian distributions):

$$R_{\alpha \text{ Herculis}} = 460 \pm 130 R_{\odot} \quad (5)$$

$$R_{\alpha \text{ Orionis}} = 645 \pm 129 R_{\odot}. \quad (6)$$

The errors on the parallaxes are unfortunately large and lead to inaccurate linear values for the stellar radii. Yet, these values could also be used to differentiate supergiants and bright giants from regular giants. Giants with the same spectral types would have radii of a few tens of solar radii. Supergiants and bright giants therefore have radii an order of magnitude larger.

5. Effective temperatures and luminosities

Bolometric fluxes for α Orionis and α Herculis have been determined by several authors and are generally compatible. We have performed estimates of the bolometric fluxes independent of these earlier values. Data to achieve this are sparse and from different sources. Methods to perform the calculation are also different. It is therefore interesting to get independent values. We have computed bolometric fluxes from infrared data listed in the 1999 edition of the Gezari et al. (1993) catalog available at CDS. The data have been complemented by *UBVR* data from the Simbad database. The data have been fitted by a blackbody Planck function to derive a bolometric flux. In the case of α Orionis, data above $5 \mu\text{m}$ have been rejected in computing the temperature, as they are dominated by circumstellar dust emission – the flux reradiated by the dust is added back in to the total luminosity below, by estimating the energy lost to absorption. No clear circumstellar dust emission is detected in the case of α Herculis and all available data have been used. In order to derive a realistic error bar on the bolometric flux, we

have associated an ad hoc common error bar to each photometric measurement by forcing the reduced χ^2 to 1. Two parameters are constrained by this fitting procedure: a scaling factor proportional to the total stellar flux and a temperature. Errors computed on these two parameters are used to derive an error on the bolometric flux by a Monte-Carlo method. This procedure takes into account the average measurement uncertainty and the photometric variability of the object as the measurements span different epochs.

Although the two sources are quite close, evidence for interstellar reddening has been investigated. There is no significant influence of the interstellar medium below 80 pc. We have used the survey by Perry & Johnson (1982) up to 300 pc and rescaled them to distance to assess the amount of reddening in volumes close to α Orionis and α Herculis. There is no significant reddening for Betelgeuse, the maximum visual extinction being on the order 0.04 after eliminating inconsistent values. The same procedure was applied to α Herculis and a mean visual extinction of 0.128 was adopted.

Evolved stars may also have circumstellar dust causing reddening. There is no evidence of reddening for α Herculis as no infrared excess is detected from the IRAS fluxes and since the $[B - V]$ color index is compatible with the intrinsic color of an M 5 supergiant given in Johnson (1966). We have assumed that the source of extinction is diffuse interstellar dust and we have used the extinction law of Mathis (1990) to compute extinction at any wavelength which gives a ratio of 1.044 between the de-reddened and the reddened bolometric flux for a temperature of 3300 K.

In the case of Betelgeuse, circumstellar dust signatures are clearly visible above $10 \mu\text{m}$ and reddening by the circumstellar

dust needs to be corrected. We have applied the procedure used in Dyck et al. (1992) who derive a visual extinction of 0.5. This results in a factor of 1.203 between the visual de-reddened and reddened bolometric fluxes.

The bolometric fluxes and associated errors are listed in the table below. We end with values very close to those used by Dyck et al. (1992) and Benson et al. (1991) which were of 40.9 and $108.3 \times 10^{-13} \text{ W cm}^{-2}$ for α Herculis and α Orionis respectively.

The effective temperature is determined by assuming that the star radiates as a black body and has a physical diameter given by its limb darkened disk diameter. The effective temperature is then:

$$T_{\text{eff}} = 7400 \left(\frac{F_{\text{bol}}}{10^{-13} \text{ W cm}^{-2}} \right)^{1/4} \left(\frac{1 \text{ mas}}{\varnothing_{\text{LD}}} \right)^{1/2} \text{ K.} \quad (7)$$

The effective temperature estimates derived from the diameters and bolometric fluxes and luminosities are listed in the following table:

Star	F_{bol} ($10^{-13} \text{ W cm}^{-2}$)	T_{eff} K	$\text{Log} \frac{L_*}{L_{\odot}}$
α Orionis	111.67 ± 6.49	3641 ± 53	4.80 ± 0.19
α Herculis	$42, 62 \pm 4.15$	3285 ± 89	4.30 ± 0.30

The luminosity is exactly as expected from Allen (2000) for the supergiant α Orionis but is much too low for α Herculis. The discrepancy for α Herculis is probably due to a lack of data for this very red supergiant class as the luminosity estimate reported in Allen (2000) for an M 5 type seems inconsistent with that for an M 2. We have adopted the limb darkened disk diameter values derived from the linear model. The effective temperature of both stars is systematically low by 100–150 K compared to the effective temperature expected for giants with similar spectral types (see e.g. Perrin et al. 1998). Such an effect has already been reported (Dyck et al. 1992). The magnitude of the effect is here shown to be somewhat smaller than seen in previous work with classical beam combiners. This systematic effect might be either due to a systematic error on the diameter which should then be underestimated by 7–8% or on the bolometric flux which should be overestimated by 15–17%. Such a big difference on the bolometric flux does not seem likely. Errors may arise from the computation of the de-reddened flux. Yet, in the case of α Herculis, the correction is only 4% and cannot be invoked to explain this effect. An underestimation of the limb-darkening by 7% would require a huge amount of darkening which is not predicted by the models and is not detected in the visibility data. Besides, limb-darkening coefficients decrease with temperature and an increase in limb-darkening should be inconsistent with an increase in effective temperature. We therefore think that the temperature of these supergiants (or bright giants) is systematically lower than that of giants of same spectral type.

The diameters we find are among the smallest in the range of diameters measured so far (Fig. 1). This suggests that the K band measurements see deeper in the atmosphere than the measurements at longer or shorter wavelengths. This is qualitatively consistent with the fact that the K band is adjacent to the

1.6 μm continuous opacity minimum, though the surprisingly large increase in apparent diameter to longer and shorter wavelengths remains to be understood and is discussed further below. Noting that since the flux distribution is strongly peaked in the near IR, it appears that the apparent size measured at these wavelengths is likely to be most representative of the stellar characteristics. More formally, a flux weighted mean diameter would be close to the H and K band diameters. This lends strong support for establishing effective temperatures based on these diameter measurements.

6. Comparison with longer wavelength data

The K and L band diameters found by our group are identical to within the errors of differential wavelength calibration between TISIS and FLUOR. We have used the L band measurement of March 2000 reported in Chagnon et al. (2002). The diameter of $42.73 \pm 0.02 \text{ mas}$ is slightly smaller than the K band diameter but we think this is due to the poorer L band calibration and to the much larger uncertainty on effective wavelength. This situation of very close diameters in K and L is dramatically different from what we have found for Mira type stars, and can be compared to what could be expected for non pulsating giant stars. Yet, in the case of Betelgeuse, measurements at 11.15 μm by Weiner et al. (2000) show a visibility curve very similar to that expected of a photosphere with a diameter 25% larger than the diameter we find at two shorter wavelengths. Two different explanations may be invoked. The first one would be that the limb-darkening might be very strong at shorter wavelengths mimicking a much smaller apparent diameter. This is the explanation of Weiner et al. (2000). However, this is not compatible with the value of limb-darkening we find in the K band and with the shape of the visibility curve which should be very much altered by such a huge effect.

Another possibility may be suggested from the study of the atmosphere of Mira stars. We have observed the brightest Mira stars both in the L band (Mennesson et al. 2002) and in the molecular and continuum bands in K (Perrin et al. 2004a). We have shown that the visibility data could be understood in all bands if a warm molecular layer were added around the star. Because of the huge amount of gas around Mira stars (perhaps elevated by dynamical effects associated with pulsation), the apparent diameters in the K and L bands are very different and much bigger in L due to the lower brightness contrast between the molecules and the photosphere of the star. The same feature can be tentatively invoked for Betelgeuse to explain the different diameters from K and L to 11.15 μm . Narrow band near IR measurements are not yet available for Betelgeuse, but we acquired such measurements on another supergiant, μ Cep, which is similar in major respects to α Orionis, including evidence for substantial mass loss. Features similar to Mira stars were detected in the visibility measurements of μ Cep (Perrin et al. 2004b). This may also apply to Betelgeuse. As a consequence, we have chosen to portray the model as a molecular layer in the following, which appears consistent with other evidence. An interpretation in terms of dust would also be possible.

The dust would require a combination of special properties, including high sublimation temperature and/or strongly wavelength dependent albedo and emissivity – e.g. McCabe (1982) – in order to survive close to the photosphere. These properties might be possible, but are not consistent with currently favored ideas of the nature of circumstellar material. Should dust prove to contribute to the layer opacity, this would not change the overall conclusions of this study with respect to analysis of the visibility measurements and the results for the photospheric dimensions and temperature.

We have used the original ISI data at $11.15 \mu\text{m}$ kindly provided by Weiner. In their article, the visibilities are modeled by a uniform disk visibility function times a constant A smaller than 1 to take into account the low frequency energy of the dusty environment. The dust is too cold and too far to be seen in the K and L bands (Schuller et al. 2004). We have therefore rescaled the original visibilities at $11.15 \mu\text{m}$ by dividing them by the factor A which is equivalent to a good approximation in this range of spatial frequencies to ignoring the radiation of the dust. We then have searched for a solution to reproduce the K , L and $11.15 \mu\text{m}$ data consistently. We have used a simple shell model of a photosphere with a uniform spatial brightness distribution and a spherical layer of zero geometrical thickness whose optical thickness is τ . τ is allowed to vary from one band to the other. The photosphere and spherical layer diameters are \varnothing_\star and $\varnothing_{\text{layer}}$ respectively. Similarly the respective temperatures are T_\star and T_{layer} . The model therefore has seven independent parameters. We have minimized a χ^2 to find the parameters that best fit the data:

$$\chi^2 = \sum_{i=1}^N \left[\frac{V_i^2 - M(\varnothing_\star, \varnothing_{\text{layer}}, T_\star, T_{\text{layer}}, \tau_{\lambda_i}; S_i)}{\sigma_i} \right]^2 \quad (8)$$

where the model $M(\varnothing_\star, \varnothing_{\text{layer}}, T_\star, T_{\text{layer}}, \tau_{\lambda_i}; S_i)$ is obtained by taking the squared Hankel transform of the circularly symmetric intensity distribution defined as a function of the wavelength λ and of the angle θ between the radius vector and the line between the observer and the center of the star:

$$I(\lambda, \theta) = B(\lambda, T_\star) \exp(-\tau(\lambda)/\cos(\theta)) + B(\lambda, T_{\text{layer}}) [1 - \exp(-\tau(\lambda)/\cos(\theta))] \quad (9)$$

for $\sin(\theta) \leq \varnothing_\star/\varnothing_{\text{layer}}$ and:

$$I(\lambda, \theta) = B(\lambda, T_{\text{layer}}) [1 - \exp(-2\tau(\lambda)/\cos(\theta))] \quad (10)$$

otherwise. This simple model is also defined in Scholz (2001) to illustrate the impact of the circumstellar environment on the center to limb variation. Although it is a quite simple view of the atmosphere of an evolved object it is very convenient to use as it only depends on a small number of parameters and allows relatively easy and quick computations.

The visibilities measured in the second and third lobes of the K band visibility function have not been taken into account for the fit in order not to bias the fit with a particular limb darkening solution. As we have seen previously, the model should be integrated in the whole band if these data are to be taken into account. The model here is computed at the effective wavelength only and mainly aims at reproducing the wavelength variations of visibilities.

The hypersurface described by the χ^2 is complex and has a large number of local minima. The variations of the hypersurface with respect to the optical depth parameters are locally convex so that the convergence with respect to these three parameters is very quick. Our algorithm explores the $(\varnothing_\star, \varnothing_{\text{layer}}, T_\star, T_{\text{layer}})$ space and finds the optimum set of optical depths for each point in this space and then chooses the full set of parameters that lead to the smaller χ^2 . In order to eliminate non physical solutions we have first linked \varnothing_\star and T_\star to keep the bolometric flux emitted by the photosphere constant. These two parameters were then set independent for the search of the final solution. The uncertainties on the parameters were computed by varying the optimum χ^2 by 1. The values we have found for the best fit parameters are listed below:

$$\begin{aligned} \varnothing_\star &= 42.00 \pm 0.06 \text{ mas} , & T_\star &= 3690 \pm 50 \text{ K} \\ \varnothing_{\text{layer}} &= 55.78 \pm 0.04 \text{ mas} , & T_{\text{layer}} &= 2055 \pm 25 \text{ K} \\ \tau_K &= 0.060 \pm 0.003 \\ \tau_L &= 0.026 \pm 0.002 \\ \tau_{11.15 \mu\text{m}} &= 2.33 \pm 0.23. \end{aligned}$$

The best fit visibility curves are represented in Fig. 7. The model reproduces the observed K and $11.15 \mu\text{m}$ data quite well. The values of the parameters are interesting. Qualitatively, a star appears larger when seen through an absorbing layer with thermal emission. Consequently, we find a smaller diameter for the photosphere of Betelgeuse than with a classical limb-darkened disk model. The effective temperature is therefore larger and compatible with the temperature of an M 1.5 star. The diameter of the photosphere is mostly constrained by the K and L band data whereas that of the layer is constrained by the ISI data. The apparent diameters in K and L are adjusted with the optical depths at these wavelengths. Their magnitude being small, the apparent diameter of the star is very sensitive to them hence their excellent statistical accuracy. This statistical accuracy is physically questionable as we think the L band data are not as well calibrated as the K band data. On the contrary, the $11.15 \mu\text{m}$ optical depth being so large it is not so well constrained as the apparent diameter of the star at this wavelength is not as sensitive to it. Taking this model into account, the set of fundamental parameters for Betelgeuse is therefore:

$$\begin{aligned} R_{\alpha \text{ Orionis}} &= 620 \pm 124 R_\odot \\ T_{\alpha \text{ Orionis}} &= 3690 \pm 50 \text{ K}. \end{aligned} \quad (11)$$

The layer is found less than half a stellar radius above the photosphere and its temperature is about 2000 K. The physical significance of the temperature is not clear, since the nature of the associated opacity is not certain.

Of course with a several parameter model, it may not be surprising that a fit to several data sets could be obtained. To underline the plausibility of this model, it is also important to appeal to other possibly related results. Numerous studies have given evidence for a high molecular atmosphere around Betelgeuse. We note that our derived temperature, 2000 K, is in agreement with the temperature of $1500 \pm 500 \text{ K}$ of a water layer described by Tsuji (2000). Unfortunately no distance for the water layer could be determined by Tsuji. The optical depths in the K and L band are very small whereas it is quite

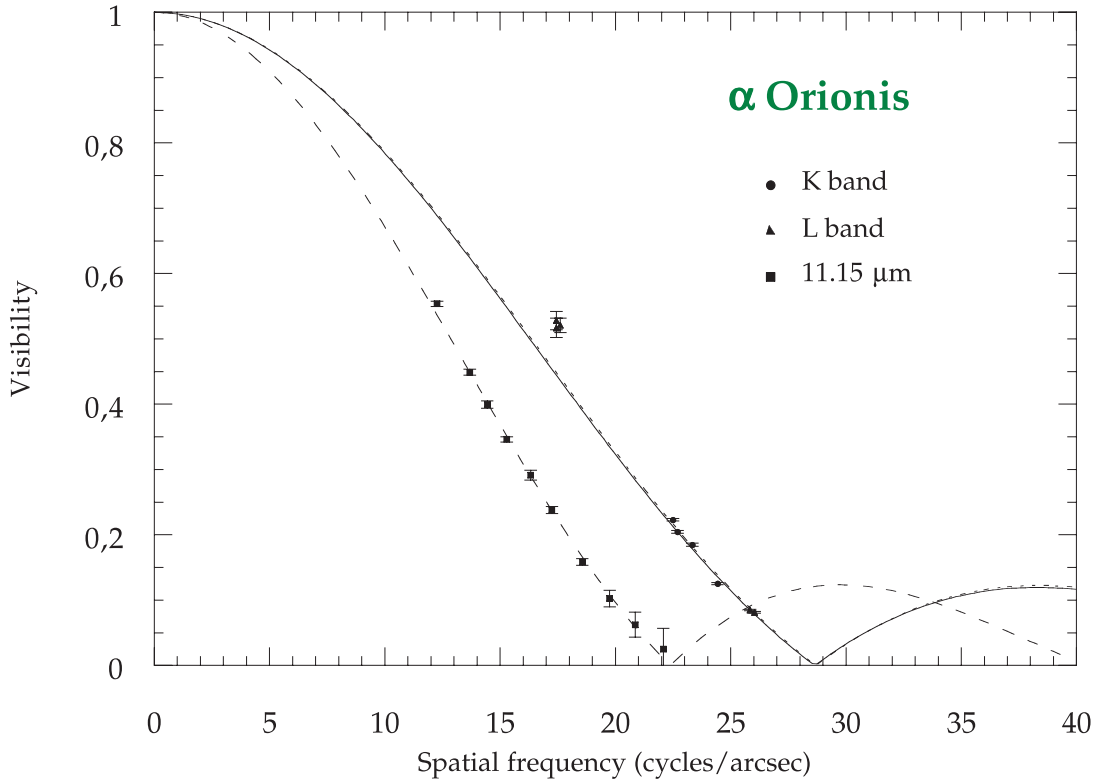


Fig. 7. Fit of α Orionis K , L and $11.15 \mu\text{m}$ data by a photosphere plus layer model. The $11.15 \mu\text{m}$ data have been rescaled to eliminate the contribution of dust (see text). Fits of the K , L and $11.15 \mu\text{m}$ data are respectively the continuous, dotted and dashed lines. Low frequency data in the L band around 18 cycles/arcsec poorly contribute to the fit which is more constrained by the better calibrated data at 26 cycles/arcsec.

important at $11.15 \mu\text{m}$. Water vapor modeled for temperatures smaller than the photospheric temperature is an absorbant at $11.15 \mu\text{m}$ whereas its absorption can be neglected at the temperature of the photosphere (Decin 2000), Weiner et al. (2000) only considered this last possibility to conclude that water vapor opacity was negligible in their study. Silicon monoxide is also a contributor to opacity at $11.15 \mu\text{m}$ and is negligible in K and L . The contribution of water vapor to opacity is also smaller at shorter wavelengths in the K and L bands. Thus molecules may be a strong candidate for the shell opacity.

The consistent modeling of interferometric measurements of α Orionis in the K and L bands and at $11.15 \mu\text{m}$ is the primary new result presented here. The success of the shell model in understanding the relation of near-IR and mid-IR measurements may be qualitatively compatible with the short wavelength measurements also. We note first that the visible and mid-IR apparent diameters are similar. It appears difficult to escape the conclusion that the atmosphere of α Orionis is greatly extended, as in the case of the mira stars. In fact, this result is not unexpected, as it has been seen with lunar occultation observations of the M supergiant α Sco (Schmidtke et al. 1989). The upper atmospheric layers (which we approximated as a thin shell) likely have both scattering and absorptive opacities which vary with wavelength. Coupled with the dependence of the Planck function on wavelength, a rich range of appearances may be observed. The spotted appearance seen at short wavelengths may scarcely appear in the infrared, due to the reduced Planck contrast.

Since the brightness distribution across α Orionis is almost certainly not properly described with a simple uniform or darkened disk model, the limb darkening derived in Sect. 4.1 does not necessarily describe the brightness distribution of the photospheric layer, and it may not be applicable to the photospheric component alone. In spite of the uncertainty in the limb darkening, it is already clear that the shell model leads to an effective temperature which is consistent within measurement errors with the T_{eff} of giants of similar spectral type. We are not able at this time to conclude that the low apparent T_{eff} of supergiants is an artifact of the outer atmospheric layers, but it must be admitted as a possibility. A similar multiwavelength analysis of additional stars will be needed (for α Herculis, the required mid-IR data is not available). Eventually, of course, it will be necessary to interpret such measurements in the context of models which successfully reproduce the large atmospheric extent.

7. Conclusions

We have been able to measure accurate diameters in the K band for α Herculis and Betelgeuse. The quality of the calibration of the visibilities sets the current limit of the absolute accuracy with a single-mode fiber interferometer like FLUOR to 0.2%. A slight change of diameter of 0.4 mas for α Herculis has been measured between 1996 and 1997, but it is impossible to guess the nature of this diameter change which may be due either to a physical increase or to a change of opacity of

the atmosphere. Visibility data acquired above the first null of the visibility functions allowed us to constrain linear and power law limb-darkening coefficients. The value found for α Herculis is in agreement with predictions whereas the disk of α Orionis shows very little darkening. The diameters measured are among the smallest in the observed range of wavelengths, most likely meaning that we see deeper in the atmosphere of these stars in the K band. The data are compatible, although they are sparse, with circular symmetry and there is no clear evidence of departure from circular symmetry due to the presence of spots detected at shorter wavelengths. This is in agreement with the result from Young et al. (2000) who found no spot signature at 1290 nm which can be explained by a lower contrast with an increasing wavelength between the Planck function brightness of the photosphere and of the atmosphere. A consistent analysis of the α Orionis data in the K and L bands and at $11.15 \mu\text{m}$ has been conducted. The three sets of data can be explained with a model comprising a 3690 K photosphere and a 2055 K warm layer located $0.33 R_{\star}$ above the photosphere. This analysis strengthens our interpretation of the direct measurement of the photospheric diameter in the K band and establishes for α Orionis an effective temperature consistent with the giant stars of the same spectral type. A consistent scenario to explain the observations of this star from the visible to the mid-infrared can be set-up. The star is seen through a thick, warm extended atmosphere that scatters light at short wavelengths thus slightly increasing its diameter. The scatter becomes negligible above $1.3 \mu\text{m}$. The upper atmosphere being almost transparent in K and L – the diameter is minimum at these wavelengths where the classical photosphere can be directly seen. In the mid-infrared, the thermal emission of the warm atmosphere increases the apparent diameter of the star.

These measurements show that optical interferometry is now well capable of exploring the limb darkening and atmospheric extension of bright, high luminosity stars. In the case of giants and supergiants, it is now possible to critically evaluate the adequacy of existing models to account for the atmospheric structure, and to determine for which stellar temperatures and luminosities the use of static models breaks down. With the increasing capabilities of optical interferometry, we can expect future measurements to record spatial measurements with higher spectral resolution and spectral coverage, better evaluating opacity sources and probing the depth dependence of the atmospheric conditions, and directly observing stellar atmospheric inhomogeneities and variations.

Acknowledgements. The authors first wish to thank T. Verhoelst for pointing to the work of L. Decin. The authors are also very grateful to J. Aufdenberg for his careful reading of the paper and for his constructive comments. Lastly, the authors are indebted to the referee whose interactions have improved the quality of this work.

References

- Allen, C. W., in *Astrophysical Quantities*, 4th edition, ed. A. N. Cox
 Benson, J. A., Dyck, H. M., Mason, W. L., et al. 1991, *AJ*, 102, 2091
 Bester, M., Danchi, W. C., Degiacomi, C. G., Townes, C. H., & Geballe, T. R. 1991, *ApJ*, 367, L27
 Browne, J. M. 2002, *Probalistic Design Course Notes*, available at <http://www.ses.swin.edu.au/homes/browne>
 Burns, D., Baldwin, J. E., Boysen, R. C., et al. 1997, *MNRAS*, 290, L11
 Chagnon, G., Mennesson, B., Perrin, G., et al. 2002, *AJ*, 124, 2821
 Claret, A. 2000, *A&A*, 363, 1081
 Cohen, M., Witteborn, F. C., Carbon, D. F., et al. 1996, *AJ*, 112, 2274
 Coudé du Foresto, V., Ridgway, S. T., & Mariotti, J.-M. 1997, *A&AS*, 121, 379
 Decin, L. 2000, Ph.D. Thesis, Katholieke Universiteit Leuven, Synthetic spectra of cool stars observed with the Short-Wavelength Spectrometer: improving the models and the calibration of the instrument
 Di Benedetto, G., & Rabbia, Y. 1987, *A&A*, 188, 114
 Dyck, H. M., Benson, J. A., Ridgway, S. T., & Dixon, D. J. 1992, *AJ*, 104, 1982
 Gezari, D. Y., Schmitz, M., Pitts, P. S., & Mead, J. M. 1993, *NASA Reference Publ.*, 1294
 Goodman, W. G. 1985, *Statistical Optics* (John Wiley & Sons Editors)
 Hestroffer, D. 1997, *A&A*, 327, 199
 Johnson, H. L. 1966, *ARA&A*, 4, 193
 McCabe, E. M. 1982, *MNRAS*, 200, 71
 Mathis, J. S. 1990, *ARA&A*, 28, 37
 Mennesson, B., Mariotti, J. M., Coudé du Foresto, V., et al. 1999, *A&A*, 346, 181
 Mennesson, B., Perrin, G., Chagnon, G., et al. 2002, *ApJ*, 579, 446
 Mozurkewich, D., Johnston, K. J., Simon, R. S., et al. 1991, *AJ*, 101, 2207
 Perrin, G. 1996, Ph.D. Thesis, Université Paris 7, A fibered beam-combiner for the IOTA interferometer. Application to the study of late-type stars
 Perrin, G., Coudé du Foresto, V., Ridgway, S. T., et al. 1998, *A&A*, 331, 619
 Perrin, G. 2003a, *A&A*, 400, 1173
 Perrin, G. 2003b, *A&A*, 398, 385
 Perrin, G., et al. 2004a, in preparation
 Perrin, G., et al. 2004b, in preparation
 Perry, C. L., & Johnston, L. 1982, *ApJS*, 50, 451
 Perryman, M. A. C. 1997, *A&A*, 323, L49
 Schmidtke, P. C., Africano, J. L., & Quigley, R. 1989, *AJ*, 97, 909
 Scholz, M. 2001, *MNRAS*, 321, 347
 Schuller, P., Salomé, P., Perrin, G., et al. 2004, *A&A*, 418, 151
 Traub, W. A. 1998, *SPIE*, 3350, 848
 Tsuji, T. 2000, *ApJ*, 538, 801
 Tuthill, P. G., Haniff, C. A., & Baldwin, J. E. 1997, *MNRAS*, 285, 529
 Van Hamme, W. 1993, *AJ*, 106, 2096
 Von der Luhe, O. 1997, in *Science with the VLT Interferometer*, ed. F. Paresce (Garching: ESO), 303
 Weiner, J., Danchi, W. C., Hale, D. D. S., et al. 2000, *AJ*, 544, 1097
 Young, J. S., Baldwin, J. E., Boysen, R. C., et al. 2000, *MNRAS*, 315, 635